Accepted Manuscript

Title: Sensitivity of Ti-6Al-4V components to oxidation during out of chamber Wire + Arc Additive Manufacturing

Authors: M.J. Bermingham, J. Thomson-Larkins, D.H. St. John, M.S. Dargusch

PII: S0924-0136(18)30119-5
DOI: https://doi.org/10.1016/j.jmatprotec.2018.03.014
Reference: PROTEC 15684

To appear in: *Journal of Materials Processing Technology*

Received date: 3-10-2017
Revised date: 22-2-2018
Accepted date: 18-3-2018

Please cite this article as: Bermingham MJ, Thomson-Larkins J, St. John DH, Dargusch MS, Sensitivity of Ti-6Al-4V components to oxidation during out of chamber Wire + Arc Additive Manufacturing, *Journal of Materials Processing Technology* (2010), https://doi.org/10.1016/j.jmatprotec.2018.03.014

Sensitivity of Ti-6Al-4V components to oxidation during out of chamber Wire + Arc Additive Manufacturing

M.J. Bermingham[a1], J. Thomson-Larkins[a], D.H. StJohn[a], M.S. Dargusch[a]

[a]*Centre for Advanced Materials Processing and Manufacturing, School of Mechanical and Mining Engineering, The University of Queensland, St Lucia, Queensland, 4072, Australia*

Abstract

Reactive metals including titanium readily oxidise and should be protected from the atmosphere during Additive Manufacturing processes. This work explores the sensitivity of Ti-6Al-4V components to oxidation contamination during out of chamber Wire + Arc Additive Manufacturing when using inert gas trailing shields. Five Ti-6Al-4V components were produced with varying argon trailing shield configurations that range from ideal inert gas shielding (resulting in no surface contamination) through to very poor inert gas shielding that results in substantial surface oxidation. Despite significant changes in the degree of surface oxide contamination between each component, the overall increase in oxygen concentration in the bulk alloys was minimal and had negligible influence on the tensile strength and ductility.

Keywords: titanium alloys; surface oxidation; additive manufacturing

[1] Corresponding author: m.bermingham@uq.edu.au,

1. Introduction

Research efforts in developing additive manufacturing (AM) technologies for producing titanium alloy components have grown considerably over recent years. A number of technologies have emerged which are suited to producing complex titanium components for aerospace, medical and other niche applications. Some titanium aerospace components can be of the order of several meters in size and one of the challenges in additive manufacturing is to produce high quality, large components as quickly as possible. Wang et al. (2013) identified Wire + Arc Additive Manufacturing (WAAM) as a potential solution because it is an out of chamber process with very high deposition rates and is an order of magnitude less expensive than powder bed AM technologies. Out of chamber WAAM involves the processing of components in natural air outside of a protective inert gas or vacuum chamber, and thus, components produced out of chamber are not limited by size unlike other AM technologies that have chamber size constraints. Wire + Arc Additive Manufacturing is based on inexpensive Gas Tungsten Arc Welding (GTAW), Gas Metal Arc Welding (GMAW) or Plasma Arc Welding (PAW) technology and uses a wire feedstock with argon gas shielding supplied through a traditional welding nozzle. Williams et al. (2016) outlined the potential for WAAM in the production of large ribbed components for aerospace applications because such components are conventionally machined from solid wrought billets and consequently there is substantial material waste. In fact in a case study evaluating additive manufactured and wrought Ti-6Al-4V aircraft brackets, Dehoff et al. (2013) found that the material cost for a complex Ti-6Al-4V machined components can exceed $1000/lb when the swarf scrap is considered. Furthermore, titanium is notoriously difficult to machine and the machining costs associated with high buy-to-fly aspect components compound the problem. Froes et al. (2007) reported that for some titanium components the cost of machining alone accounts for half of the total component cost. WAAM presents a unique opportunity for the aerospace market because it can produce large components quickly which are then subsequently finish machined to final tolerance, eliminating the expensive rough machining operations.

A very important consideration when processing titanium during liquid to solid transformations (e.g. casting, welding, additive manufacturing) is to manage the potential for atmospheric contamination, particularly oxygen. Conrad (1981) thoroughly studied the effect of interstitial oxygen, nitrogen and carbon on the properties of titanium and acknowledged titanium's extreme reactivity and strong affinity for such interstitials which cause severe embrittlement. Oxygen is an important alloy element and provides strengthening but its allowable concentration in the alloy is strictly limited. For example, ASTM Grade 5 Titanium (Ti-6Al-4V) has a maximum allowable oxygen content of 2000ppm. Preventing atmospheric contamination during melt handling can be achieved by processing under a vacuum, an inert gas chamber or by providing a localised inert gas shield. Most titanium AM processes such as Electron Beam Melting, Selective Laser Melting etc. occur in a vacuum or inert gas chamber where contamination is a non-issue. However, preventing contamination remains is an ongoing challenge for any out of chamber AM process such as WAAM.

Fundamentally, the challenges facing out of chamber AM processes are similar to those for welding. A review of out of chamber welding processes by Short (2009) concluded that prevention of atmospheric contamination is usually achieved by protecting the hot surface with a high purity argon cover gas using a trailing shield which is connected to the welding torch. A trailing shield is a localised shielding device that maintains argon shielding of the hot weld metal until it cools to a temperature where atmospheric contamination no longer presents a risk. Major titanium producers such as TIMET (1997) now recommend that it is best practice during welding processes to shield titanium until temperatures fall below approximately 400°C. Furthermore, Talkington et al. (2002) found that most experienced welding technicians use the appearance of the weld as a guide to its quality on account that titanium is discoloured when oxidized. Research findings support this common practice, for instance, Maak (1984) and Li et al. (2005) have shown a strong correlation between surface discolouration and the bulk interstitial oxygen content and the associated

detrimental mechanical properties of titanium welds. However, it is worthwhile noting that these findings are a result of contamination occurring from impure shielding gas during the melting process, which does not necessarily represent the alternative scenario where contamination only occurs post-solidification as the solid weld cools to below 400°C. Harwig et al. (2000) correctly point out that contamination in the trailing shield may result in apparent oxidation and discolouration but unless the contamination occurs while the weld is molten it is unlikely to have serious implications beyond the localised surface. This is because titanium is most vulnerable to contamination in the liquid state when diffusion occurs most rapidly. Under these circumstances contamination will result throughout the entirety of the molten pool, as opposed to highly localised surface contamination that otherwise occurs when hot solid titanium is temporarily exposed to unprotected atmospheres during cooling. Hoye et al. (2011) also concluded that surface discolouration is only representative of surface contamination and does not correlate to bulk interstitial oxygen contamination when melting and solidifying under ideal shielding conditions and then removing the shielding before cooling to room temperature. Nevertheless, surface oxidation presents a challenge for out of chamber additive manufacturing because any surface oxide will be readily dissolved and absorbed into the liquid titanium as the next layer is deposited.

There is currently limited understanding surrounding the requirements of trailing shields used for out of chamber titanium additive manufacturing processes but there is evidence that trailing shields are effective in minimising contamination during WAAM. Wang et al. (2013) used a localised trailing shield during WAAM of Ti-6Al-4V and reported a negligible 70ppm pick-up in oxygen during deposition (up from 1500ppm in the original wire) and was able to produce high quality components. Similarly, Bermingham et al. (2015) reported a 230ppm oxygen pick-up during deposition of Ti-6Al-4V (up from 700ppm in the original wire) using a commercially available shield. Ding et al. (2015) designed an improved localised shielding device that created laminar flow and

used oxygen sensors to assess its effectiveness for WAAM applications at various argon flow rates and distances from the sensors. The authors found that it was effective in displacing oxygen under a wide range of flow rates and theoretical build heights and concluded that it should be highly effective for WAAM. These studies confirm that correctly designed and installed localised trailing shields are effective in preventing contamination during WAAM but there is still little known about the susceptibility of Ti-6Al-4V is to oxidation from a poorly designed or poorly installed localised trailing shield (which may inadvertently occur in the practice of fabricating complex parts).

The purpose of this research is to investigate the quality of post-deposition inert gas shielding on changes in alloy chemistry (oxygen pickup) and tensile properties of Ti-6Al-4V components produced by Wire + Arc Additive Manufacturing. Several components are produced by the WAAM process with different trailing shield configurations ranging from complete shielding (expected to result in no contamination) through to no trailing shield being used (expected to result in substantial contamination). The effectiveness of using bead blasting techniques as a method to remove contaminated surfaces between layers in an attempt to improve the quality of poorly shielded components produced by WAAM is also explored.

2. Experimental

The Wire + Arc Additive Manufacturing technique was used for this study (details about the equipment and base experimental set up are available in Mereddy et al. (2017)). In summary, the process uses a CNC controlled Gas Tungsten Arc Welding (GTAW) torch and automated wire feed to deposit layers. Ti-6Al-4V wire was used as the feedstock (initial composition: 5.95wt% aluminium, 4.02wt% vanadium, 0.07wt% oxygen) and a wrought Ti-6Al-4V base plate was used as a substrate for the deposits. A custom manufactured trailing shield was used in this study and this involved flowing

high purity argon (99.999%) through a 5mm thick porous sintered stainless steel plate (Figure 1). The argon flow rate was 10L/min through the GTAW torch and 10L/min through the trailing shield (20L/min combined). The trailing shield attached to the welding torch provided shielding for approximately 140mm length of deposited layer.

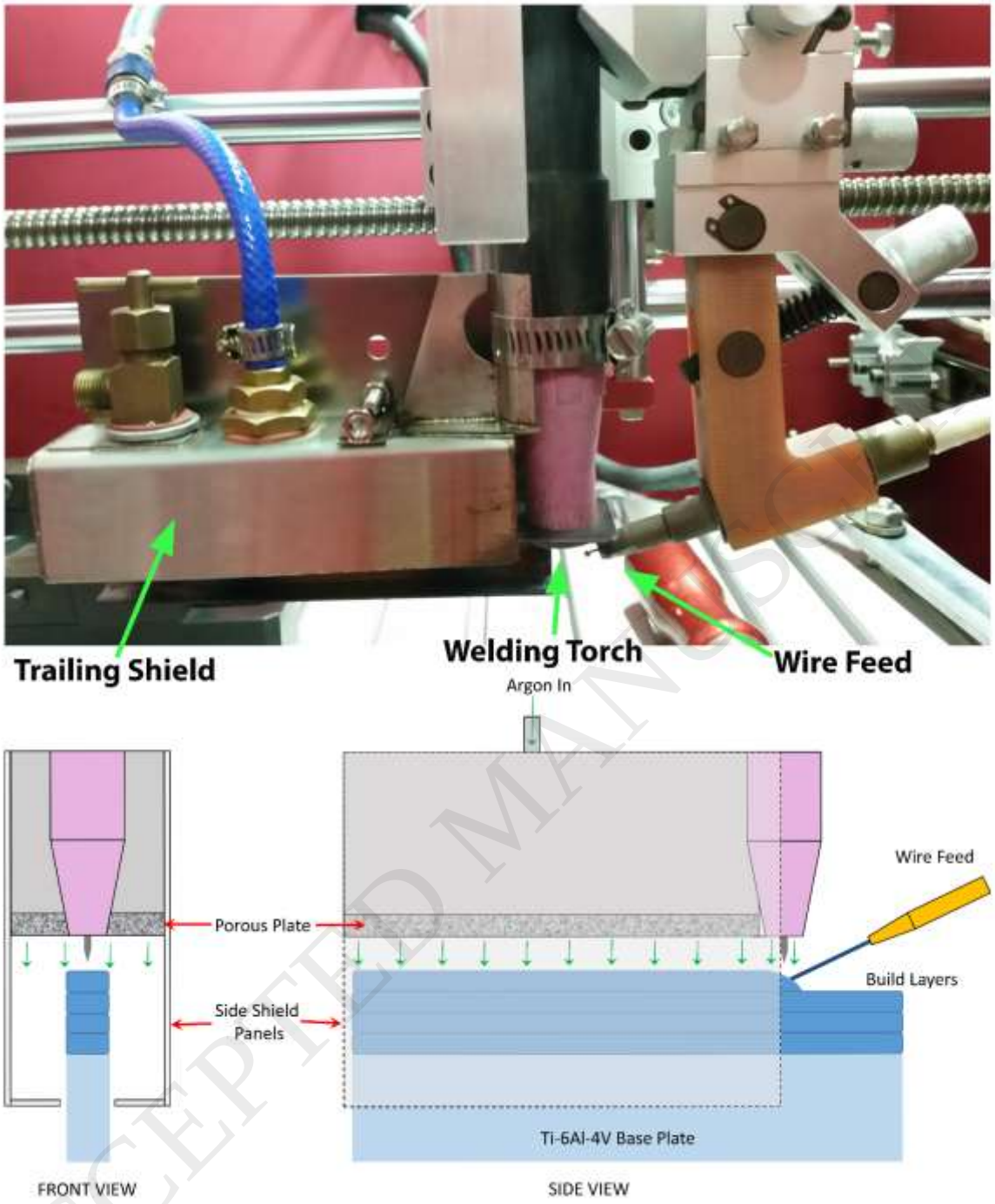

Figure 1. Photograph and schematic of the trailing shield used during Wire + Arc Additive Manufacturing. Note that the side shield has been removed in the photograph. Under the ideal shielding test condition, the porous plate is in line with the welding torch nozzle and the side shields have a lower bracket that almost touches the base plate (i.e. 1-2mm of clearance between the side shield panels and the base plate), creating a chamber around the cooling metal.

Each deposit was created by moving the welding torch in a linear direction and feeding wire into the molten pool, which subsequently solidified to make a layer. A subsequent layer was then deposited over the first by increasing the height of the torch. To eliminate heat accumulation as a variable, the parts were permitted to cool between layers until the interpass temperature was room temperature. After this, deposition continued until the approximate dimensions of the final build was approximately 180mmx12mmx12mm (not measuring the base plate), which corresponded to four layers. Details of the deposition parameters are given in Table 1.

The temperature and cooling rate of the molten pool at the end of deposition[2] was measured using a non-contact IR pyrometer, calibrated for emissivity against ultra-high purity titanium (99.995% purity). Calibration was performed by melting a stationary pool of the high purity titanium and experimentally determining the emissivity against the measured thermal arrests occurring at known phase transformation temperatures as it cooled (L→S at 1668°C and β→α at 882°C). The average emissivity from three calibration tests was 0.2907 at the solidification temperature and 0.2909 at the β→α transformation temperature for the high purity titanium. It was assumed that the emissivity would be comparable between Ti-6Al-4V and pure titanium.

[2] The temperature was measured at the end of the layer after the arc was terminated. It was not possible to measure during deposition as the trailing shield prevented direct measurement because it enclosed the cooling metal.

Table 1. Deposition parameters used to build the components.

Deposition Parameters	
Peak Current:	150Amp
Base Current:	75Amp
Pulse:	5kHz
Wire feed:	1.5m/min
Wire:	Ti-6Al-4V, ø=1.0mm
Deposition speed:	50mm/min
Electrode-substrate gap:	5mm
Vertical build interval:	≈3mm
Substrate:	Ti-6Al-4V
Electrode:	ø=2.4mm tungsten-rare earth
Argon:	99.999% purity, 20 L/min
Torch Nozzle diameter:	19mm

To investigate the effect of the trailing shield on the quality of the Ti-6Al-4V components, five separate trailing shield configurations were tested (labelled here C1-5 and shown graphically in Figure 2). The first condition (here labelled C1) was to build under the ideal shielding scenario and involved using the trailing shield configuration shown in Figure 1 which was necessary in order to obtain a shiny 'silver' surface finish (indicating negligible oxidation). The next targeted scenario (C2) was imperfect shielding where the aim was to obtain a bluish-greenish oxide layer which indicates that some light oxidation has occurred. This was achieved by increasing the height between the trailing shield and the deposited surface to approximately 5mm above the position used under C1 (in other words, the gap between the deposited material and the porous plate of the trailing shield increased which increased the potential for air to infiltrate). The third test condition (C3) was to

deliberately introduce contamination in order to achieve poor quality shielding and involved removing the lower brackets from the trailing shield wall (effectively opening the bottom of the trailing shield to the atmosphere). The fourth test condition (C4) was identical to the third, except after deposition each layer was bead blasted to remove noticeable brown oxide. This involved transferring the component into a bead blasting unit (HAFCO SB-375 at 100psi using Potters Ballotini Glass impact beads with a maximum-minimum size range of 300µm - 180µm of with a minimum 70% of particles spherical). Bead blasting was performed for a minimum of 2 minutes, after which all flaky oxide was visibly removed giving the appearance shown in Figure 3a. The fifth and final test condition (C5) was to remove the trailing shield completely which resulted in a heavy brown flaky oxide which was retained and redeposited onto by the subsequent layer. These configurations are summarised in Table 2.

Table 2. Summary of trailing shield configurations and the surface appearance of the deposited material.

	Visual appearance of freshly deposited surface after cooling to room temperature
C1	Ideal Shielding – no oxidation/contamination (shiny surface finish on component)
C2	Light oxidation/contamination (Blue-Grey-Green surface oxide on component)
C3	Poor Shielding – strong evidence of oxidation (brown oxide, flaky)
C4	Same as ‘C3’ except Bead Blasted between layers to remove brown oxide
C5	No Trailing Shield – heavy brown oxide and very flaky

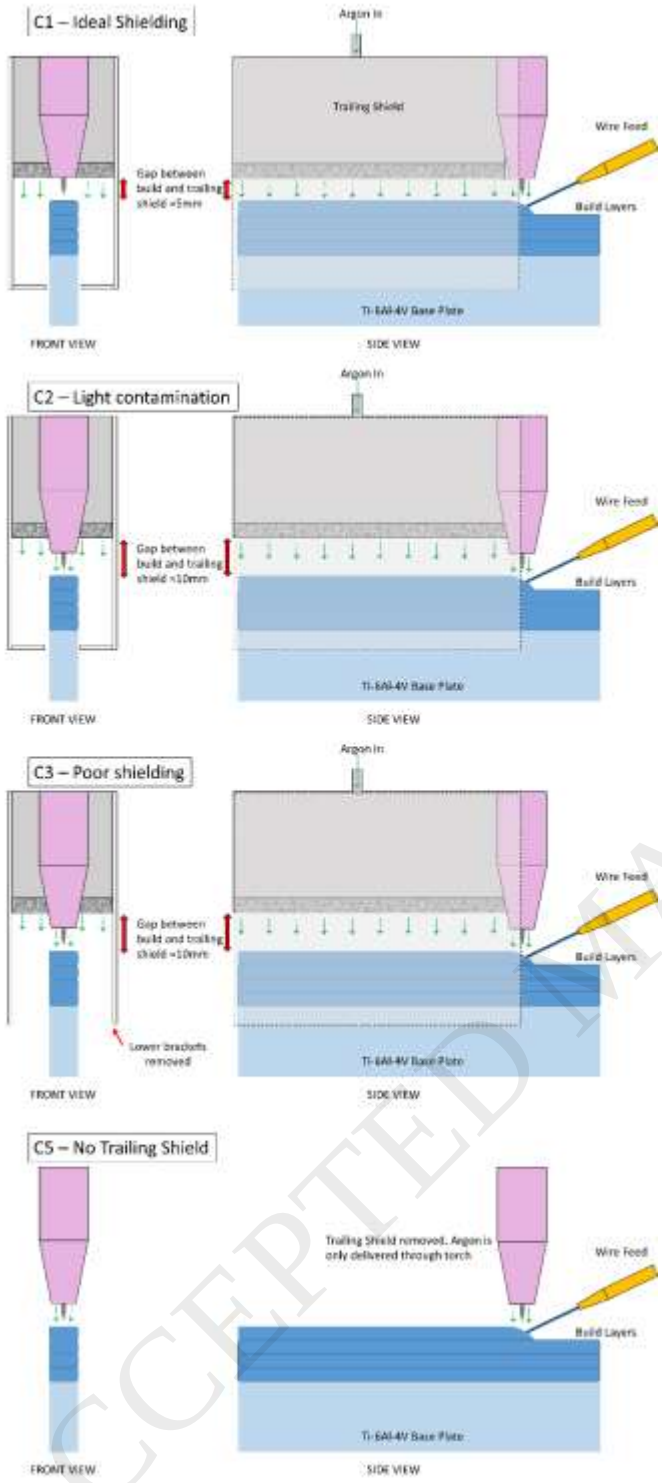

Figure 2. Schematics showing the different trailing shield configurations used (not drawn to scale). Conditions C1-C3 only have subtle variations such as the height (gap) of the trailing shield from the surface of the component and the positioning of lower brackets attached to the trailing shield. Condition C4 is the same as that presented for C3, except bead blasting was used to remove excessive surface oxide between each layer.

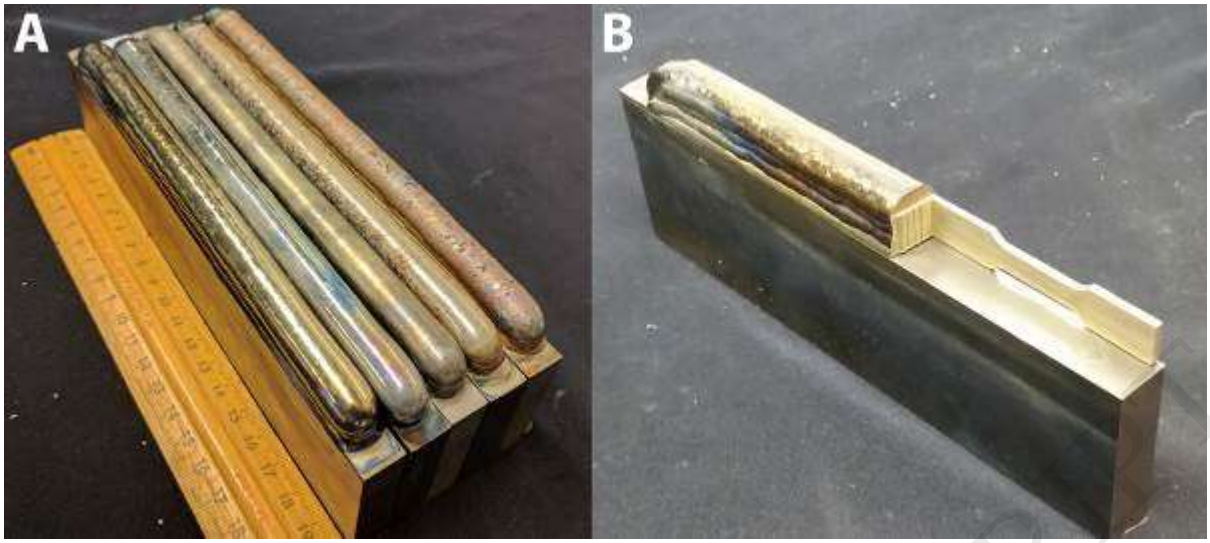

Figure 3. (A) Photographs of the samples produced by WAAM after 4 layers showing the different quality surface finishes achieved. Left to Right: C1, C2, C4, C3, C5. (B) Photograph showing the orientation of the tensile bars tested (in tension normal to the build direction).

After deposition, all components were photographed (Figure 3) and a small section removed for analysis of the surface. The remainder of the build components were stress relieved for 2 hours at 480°C before being machined into tensile bars and samples for microstructural and chemical analysis. The stress relief selected is within the effective Ti-6Al-4V stress relieving range and time recommended by Donachie (2000) for ASM International. Tensile bars were machined using modified geometries of ASTM E8M (flat dogbone, 1.5mm x 5mm gauge cross-section x 16mm gauge length) and tested at a crosshead speed of 0.5mm/min. It is well known that Ti-6Al-4V components produced by additive manufacturing can be highly anisotropic and as such, the orientation selected for testing was in the horizontal direction, which is frequently reported to be the least ductile direction in Ti-6Al-4V components manufactured by WAAM in studies previously conducted by Baufeld et al. (2010), Baufeld et al. (2011), Baufeld and Van der Biest (2009), Brandl et al. (2010), Wang et al. (2013) and Bermingham et al. (2018). Five tensile specimens were tested for each condition in this direction to assess the worst case scenario as any oxygen contamination is expected

to significantly embrittle the components. Microvickers hardness testing (50gm load, 12sec) was performed to assess the hardness variations against distance from the top surface up to a distance of 500µm. Samples were prepared for microstructural analysis using conventional processes (progressive grinding on SiC papers followed by polishing with a suspension of 90% colloidal silica (Struers OPS) + 10% H_2O_2 for 10minutes. Following polishing, the samples were etched with Krolls reagent. The microstructure was investigated using optical and electron microscopy techniques.

3. Results and Discussion

The as-deposited + stress relieved microstructure contained fine acicular α with intergranular β and there was no apparent differences in the microstructures produced by any of the different test conditions. This microstructure, including the dimensions and morphology of the α-phase is largely determined by the cooling rate and has been discussed by Bermingham et al. (2015).

The primary difference between the test conditions was the noticeable states of oxidation that had occurred on the surfaces of the components during the WAAM process. This effect of oxidation is visibly apparent by the naked eye in Figure 3 and is shown in detail via SEM in Figure 4. For conditions C1 and C2 it was easy to discern microstructural features on the surface during SEM observation but for all other conditions the oxide became so thick that no evidence of the microstructure could be resolved. The presence of oxygen in large concentrations (>40at%) was found during EDS analysis of the C3, C4 and C5 surfaces. It was clear that there were different oxide layers present with C3 and C5 showing a thick flaky oxide on top of a more robust and stable oxide layer that was not able to be removed even after bead blasting (C4). The flaky oxide is of the order of 5-10µm thick and is quite fragile with visible cracks that appear to have been propagating through it.

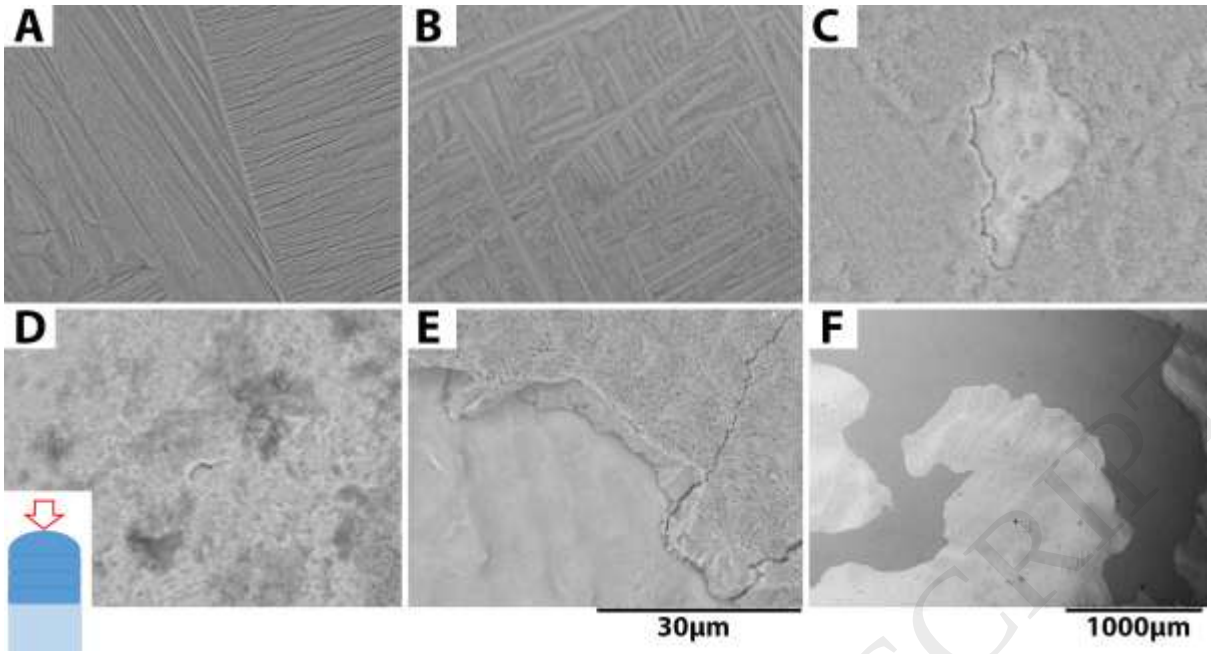

Figure 4. SEM images of the top free surfaces of the components showing the different states of oxidation: (A) C1, (B) C2, (C) C3, (D) C4, (E & F) C5. Each image shows the external surface of the top layer at its apex *(indicated by the diagram insert in D)*. Images A-E are at the same magnification while (F) shows a low magnification of C5. Colonies of α-laths and/or widmanstätten-α can be observed on the surface of C1 and C2 (indicating a very thin oxide) but the thick oxide present on all other cases prevents visualisation of microstructural α-phase features. EDS point analysis on the surface of conditions C3-C5 detected large proportions of oxygen (>40at%) which is consistent with oxide.

SEM images of the cross section revealing the top surface and the measured hardness variations with distance from the surface are shown in Figure 5. There is no significant change to the microstructure near the oxidised surfaces except for the increased roughness associated with heavy oxidation. The acicular α-lath thickness marginally increases immediately below the surface in conditions C3-C5 and could be related to the fact that α-Ti is stabilised by oxygen. This is supported by clear evidence that the hardness near the surface is significantly higher than the bulk hardness, especially in conditions C3-C5. In conditions C1 and C2 the hardness marginally increases by about 30HV above the bulk value but plateaus at depths greater than 25µm from the surface. As expected,

the highest hardness near the surface corresponded to C5 when no trailing shield was used, however, this value again plateaued to the base level between 50-100µm from the surface (although it is worth noting that this measurement does not include any oxide flake that may have detached). The use of bead blasting as an attempt to remove oxidation (C4) proved ineffective with no measureable difference between the hardness-depth values of C3 and C4. Hardness is a strong indicator for interstitial oxygen contamination and has commonly been used as a method to gauge the ingress of oxygen during heat treatments of titanium in unprotected atmospheres and to certify the quality of titanium welds. For example, Talkington et al. (2002) developed a portable titanium weld certification technique based on hardness testing. Dobeson et al. (2012) studied the rate of development of alpha case (oxide) on titanium at various combinations of temperature and time and reported that the rate of oxygen absorption is much higher in the β-phase than in the α-phase and proposed an empirical model predicting the thickness of the contaminated layer with exposure time and temperature. Interestingly, the depth of oxygen diffusion into titanium after 1 hour exposure at 1000°C was limited to about 100µm, which is similar to that measured here for C5. Given that the penetration of oxygen is somewhere between 50-100µm in C5, it is likely that the majority of contamination has occurred in the brief few seconds while the component cooled at the high temperatures above 1000°C (Figure 6). Since cooling is quite rapid (occurring over seconds), during this short period the solid state diffusion of oxygen into the alloy is limited to small distances from the surface.

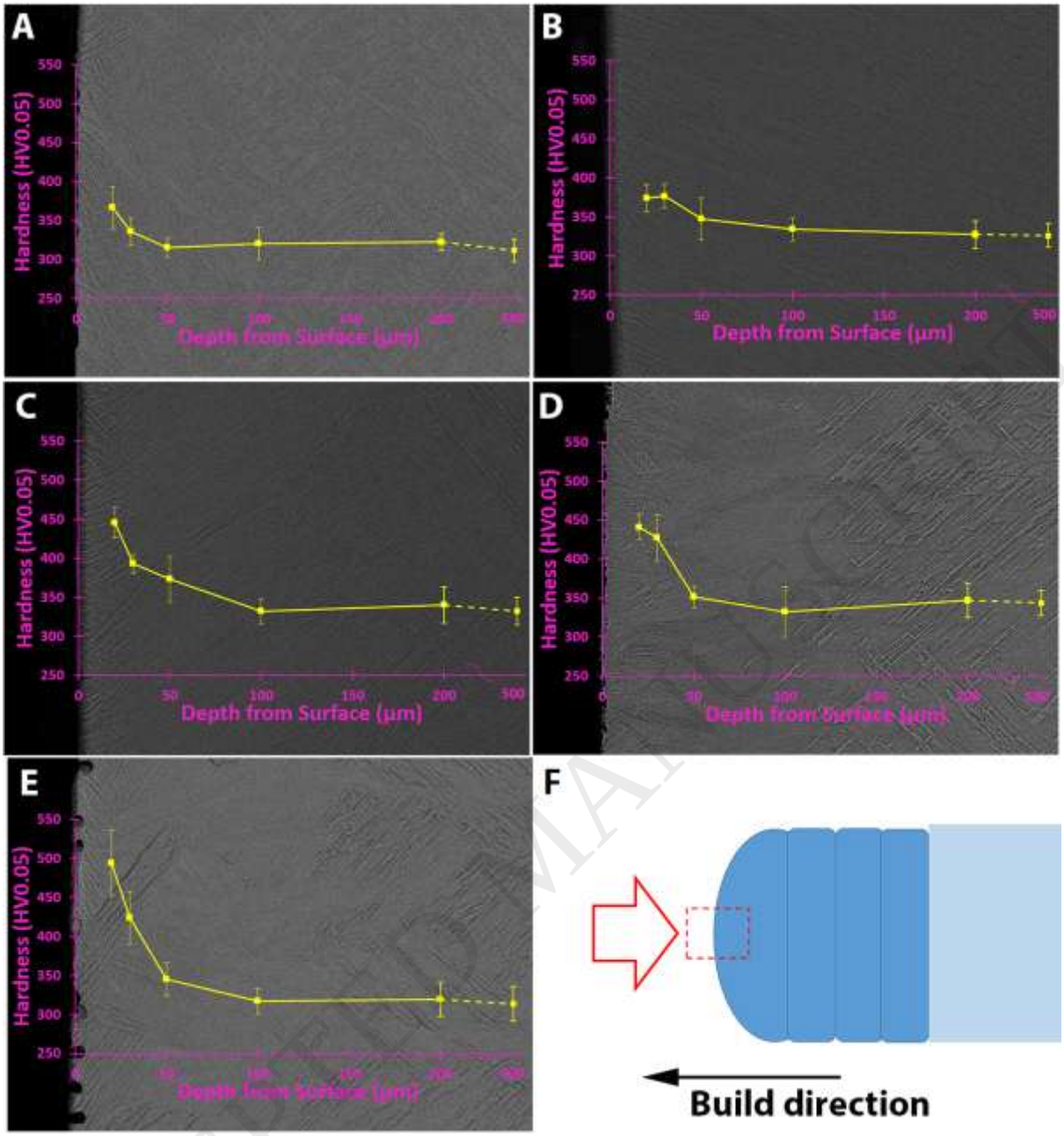

Figure 5. Microstructure at the top surface of each component as well as a sketch showing the location where these images were taken (F). (A) C1, (B) C2, (C) C3, (D) C4, (E) C5. The microhardness as a function of depth is overlayed. Each of these data points represents and average of at least 10 measurements, error bars indicate ±1 standard deviation.

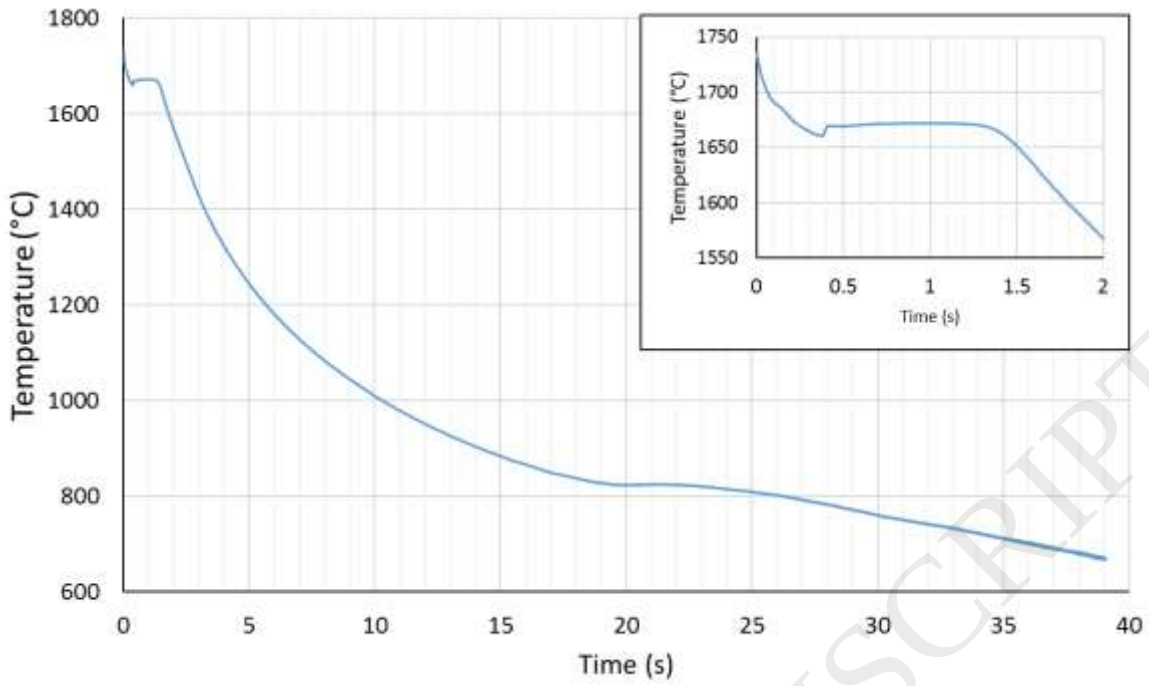

Figure 6. Cooling rate at the end of Layer 3 in C1. The cooling rate prior to solidification was approximately 90°C/s and slowed to approximately 11°C/s prior to β→α transformation. The insert shows the first few seconds of the liquid to solid transformation.

The chemical analysis as determined by LECO combustion and ICP Atomic Emission Spectroscopy for each of the test conditions is also supportive of the fact that only limited atmospheric contamination has occurred during each of the trailing shield configuration tests. The samples for chemical analysis were taken in the centre of the components more than a millimetre away from the contaminated surfaces and represent the bulk alloy concentration. The bulk concentration was an average taken from approximately 200mm^3 of material. Overall, there was limited oxygen pickup in the bulk concentration for C1-C4 which remained around the same level as the initial wire at 0.07wt%. However, the oxygen pickup in C5 (no trailing shield condition) slightly increased to 0.10wt% (an increase of 300ppm). In light of the microhardness testing it is not possible for solid state diffusion to account for this increase alone, and instead, indicates that the remelting of previously oxidised layers as new layers are deposited has likely resulted in this slight increase in bulk oxygen concentration. Nevertheless, this is well below acceptable levels and is actually half of the

acceptable tolerance for ASTM Grade 5 which sets a maximum of 0.20wt% for oxygen and furthermore, the measured level is even within the oxygen tolerance for the higher purity ASTM Grade 23 which has a maximum oxygen content of 0.13wt%. It appears that the purity of the initial wire feedstock is particularly important and is the main factor that determines the composition of the built components. Any oxides that are present on the surface appear to be completely dissolved into the bulk alloys once the next layer is deposited. Figure 7 shows the cross section through a multi-layer wall built without the trailing shield (C5) together with a higher magnification insert of the microstructure between the layers. No evidence of residual oxides or incomplete melting are observed. Columnar grains are observed to grow seamlessly across layers.

Table 3. Chemical analysis of the bulk components (measured in the centre of component away from the edge). O and N determined by LECO combustion and Al, V, Fe determined by ICP-AES. Note that the accuracy of the O and N detection is approximately ±0.01wt% and Al and V the accuracy is ±0.09wt% (these ranges represent 1 standard deviation).

	O	N	Al	V	Fe
	wt%	wt%	wt%	wt%	wt%
C1	0.08	0.007	5.73	3.63	0.11
C2	0.07	0.008	5.79	3.69	0.11
C3	0.06	0.010	5.73	3.67	0.12
C4	0.07	0.013	5.92	3.70	0.12
C5	0.10	0.011	5.9	3.73	0.08

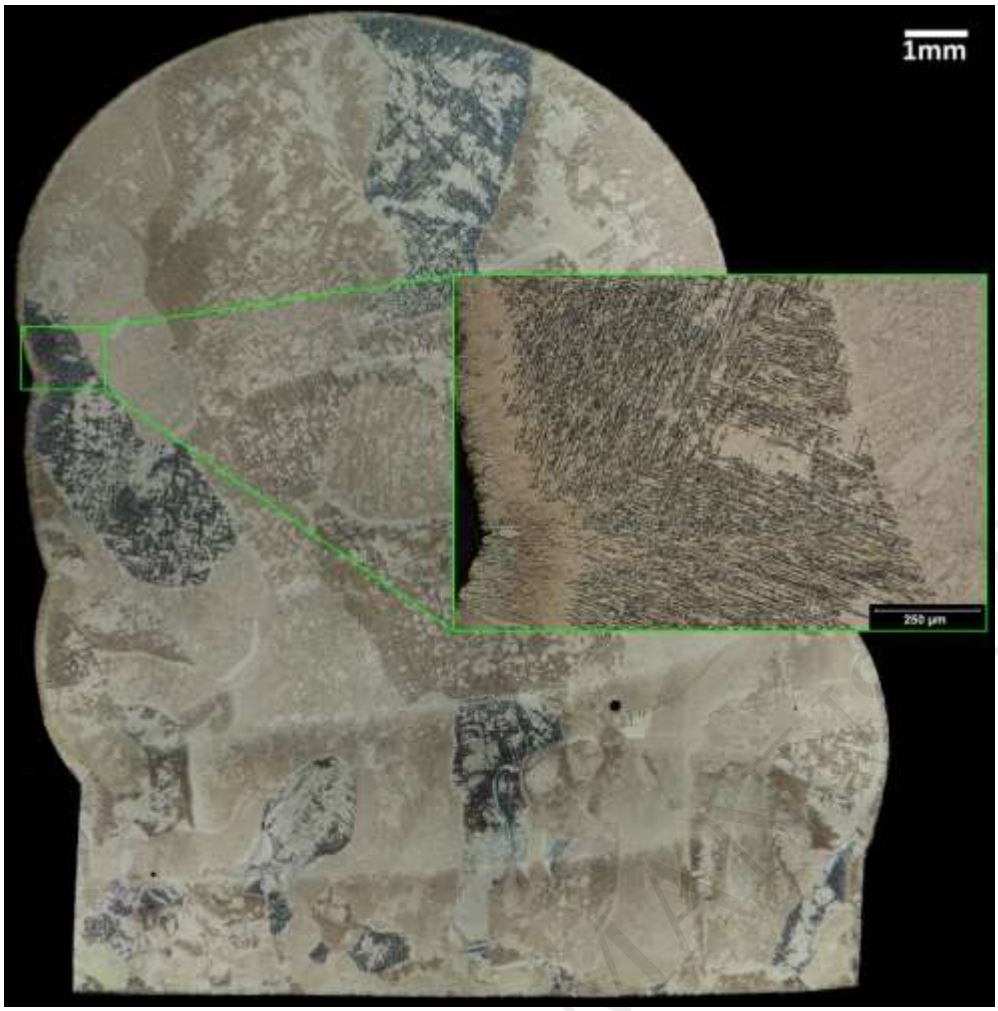

Figure 7. Cross section through C5 (no trailing shield) with higher magnification image showing the microstructure between layers. Epitaxial columnar grain growth occurs from the previous layer into the new layer and there is no visible evidence of undissolved oxides. (Note: the layers can be identified by the curvature at the sides of the wall and the insert shows a magnified area between two layers).

The result of the tensile tests are summarised in Figure 8. All test conditions meet the minimum strength and ductility requirements set out for cast Ti-6Al-4V in ASTM F1108, which requires a minimum yield strength of 758MPa and minimum elongation at failure of 8%. The tensile test results indicate that there is little difference between the strength and ductility for each trailing shield configuration, although from visual inspection of Figure 8 there appears to be a slight decrease in the ductility for condition C5 (and commensurate slight increase in tensile strength).

However, comparing data by visual inspection is highly subjective and as such, to more accurately determine if statistical differences exist between the C1 condition and all other tests, Tukey's multi-comparison test with 0.05 significance was applied. This method compares the means of each data set and determines whether a significant difference exists with 95% level of confidence. This analysis determined that there is no significant difference in the ductility, yield strength or tensile strength when comparing C1 to all other conditions at the 0.05 level (Table 4). Due to limited resources, only five tensile test specimens were prepared for each test condition and for greater confidence it would be necessary to test a larger sample size in order to better identify statistically significant differences between the ideal shielding (C1) and all other trailing shield configurations (C2-C5).

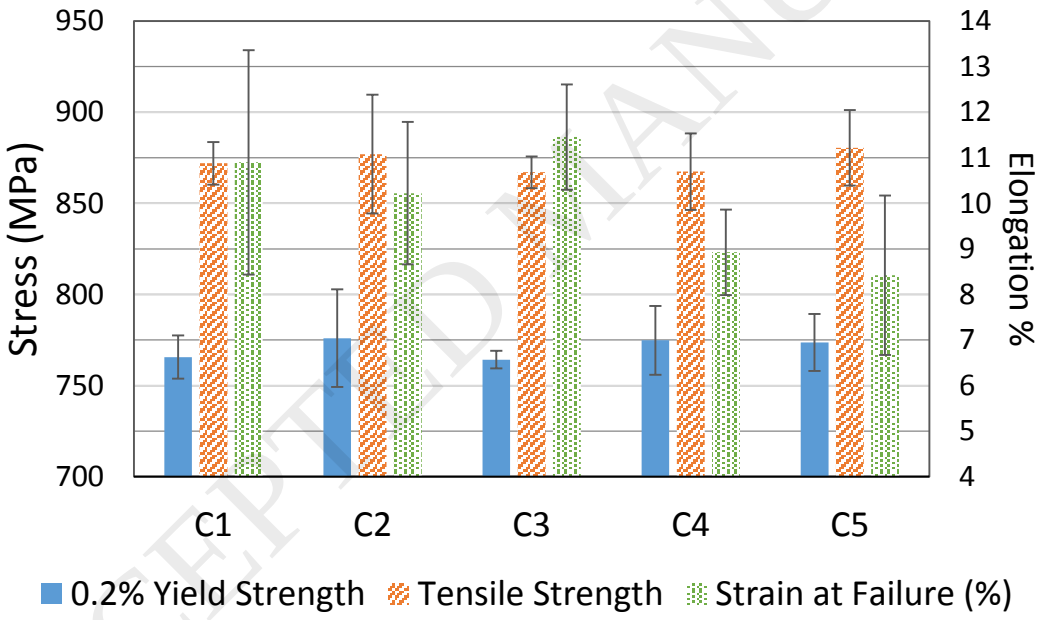

Figure 8. Average results from tensile testing 5 samples for each condition C1-C5. The error bars represent ±1 standard deviation.

Table 4. Tukey multiple comparison test for significant difference at 95% confidence level. The 0.2% yield strength, tensile strength and elongation at failure of the ideal shielding condition (C1) is compared to all other conditions and no significant difference is determined based on the sample size of 25 tensile tests.

	Dataset	Mean	Difference between means	Simultaneous Confidence Intervals		Significant at 0.05 level
0.2% Yield Strength (MPa)	C1	765.6		Lower Limit	Upper Limit	
	C2	776	-10.4	-42.91653	22.11653	No
	C3	764.2	1.4	-31.11653	33.91653	No
	C4	774.8	-9.2	-41.71653	23.31653	No
	C5	773.6	-8	-40.51653	24.51653	No
	Dataset	Mean	Difference between means	Simultaneous Confidence Intervals		Significant at 0.05 level
Tensile Strength (MPa)	C1	872		Lower Limit	Upper Limit	
	C2	877	-5	-44.22728	34.22728	No
	C3	867	5	-34.22728	44.22728	No
	C4	867.4	4.6	-34.62728	43.82728	No
	C5	880.4	-8.4	-47.62728	30.82728	No
	Dataset	Mean	Difference between means	Simultaneous Confidence Intervals		Significant at 0.05 level
Elongation at failure (%)	C1	10.898		Lower Limit	Upper Limit	
	C2	10.2228	0.6752	-2.46759	3.81799	No
	C3	11.4534	-0.5554	-3.69819	2.58739	No
	C4	8.9262	1.9718	-1.17099	5.11459	No
	C5	8.4212	2.4768	-0.66599	5.61959	No

The technique of using abrasive bead blasting between build layers in the attempt to remove oxide contamination did not result in a measurable improvement to the tensile properties or reduction in the bulk oxygen content of the components. Although the brown surface oxide was removed by this process, the technique proved ineffective in removing contaminated material resulting from the solid-state diffusion of oxygen into the titanium metal as it cools. Referring to Figure 5 it is clear that the depth of this contamination below the surface in the bead blasted condition (C4) was comparable to the condition without bead blasting (C3).

The results of the bulk chemical analysis, tensile properties and microhardness surface evaluation confirm that limited contamination occurs during the building of Ti-6Al-4V components in out of chamber WAAM using the deposition parameters investigated, even when no trailing shield was used (C5). The C5 condition represents a worst-case scenario and in practice, it is more likely that some degree of trailing shielding would be used during the fabrication of titanium components by WAAM. In such circumstances while it is important to be aware of the risk of oxidation during WAAM, it appears unnecessary to achieve an absolute perfect shiny colour-free surface finish as is generally desired during melting or heating of titanium outside of inert gas or vacuum chambers. In the present study there was practically no measurable difference between C1 (shiny surface with no discolouration) and C2 (blue-green-grey oxide) except for the visual appearance of the oxide surface colour. It is of course essential that adequate shielding be established during the melting and solidification process as any contamination here will almost certainly result in poor outcomes. If contamination occurs during the melting process itself then the trailing shield will be redundant no matter how effective it is in producing oxide free surfaces. Under certain conditions it may even be possible for oxidation to occur during melting and subsequently be reabsorbed if the trailing shield is well configured, giving the surface the appearance of a high quality component but in reality is deeply contaminated. Due to titanium's ability to dissolve its own oxide, Harwig et al. (2000) found

that this very scenario can occur during welding processes. For these reasons engineers developing industrial out of chamber WAAM processes must direct efforts to ensure that contamination does not occur during the melting process.

The ability of the molten pool to solidify while under the protective inert atmosphere offered by the welding torch depends on a number of factors some of which include the welding parameters used, the physical size of the shielded zone and alloy specific parameters such as the freezing range. Figure 9 shows a theoretical illustration of two steady state scenarios where (A) the molten pool is always confined within the shielded zone and (B) the molten pool is partially exposed to the contaminated atmosphere. Note that this representation assumes a step change between the unshielded and shielded zones, whereas in reality some outward flow of argon along the surface is likely. The key factors insuring the quality of the deposit are the length of the molten pool (determined by processing parameters) and the size of the shielded zone (determined by nozzle diameter). While it is clear that scenario (A) has occurred with the deposition parameters studied here, changes to these parameters may increase the size of the molten pool and increase the risk of contamination. Perhaps the simplest hardware modification to improve shielding (apart from adopting a trailing shield) is to increase the diameter of the welding nozzle which would provide a larger factor for safety for a range of deposition conditions.

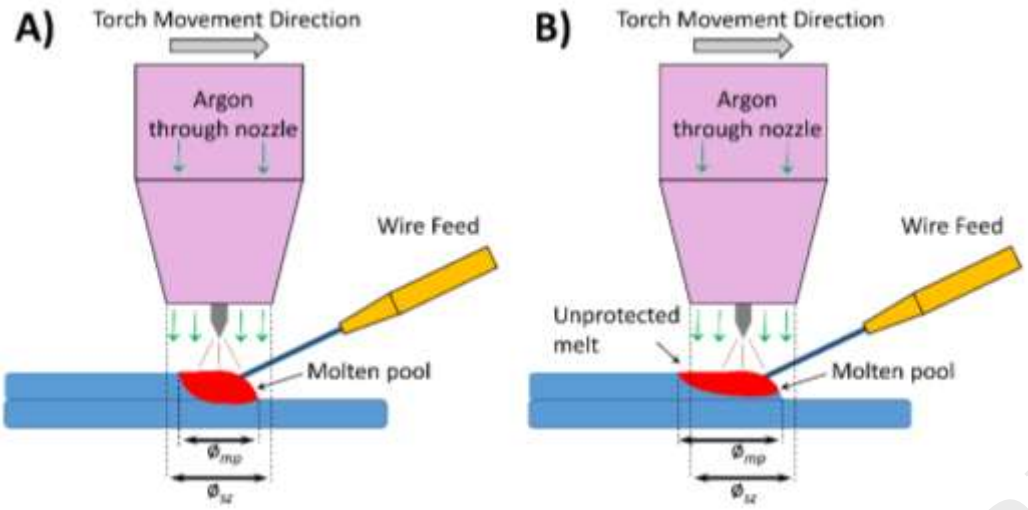

Figure 9. Schematic representation of two steady state WAAM building scenarios. In (A) solidification occurs before the molten pool exits the protected shielded zone (*øsz*) and therefore no continuation occurs when the metal is liquid. The alternative scenario (B) is where the combination of experimental and alloy specific parameters result in the melt pool not completely solidifying before it exits the shielded zone. The second scenario (B) must be avoided at all costs because atmospheric contamination will occur rapidly and likely result in unacceptable oxygen pickup. For simplicity, a step change between zones of complete shielding and complete non-shielding has been depicted but in reality there is likely to be a mixed zone at the periphery of the shielded zone.

One of the important findings of this study is that the chemical composition of the wire feedstock is critical in producing high quality components by WAAM when solidification occurs under a protected cover gas. There was limited oxygen pickup during processing and the final composition was almost entirely dependent on the wire's initial oxygen content. Therefore although it is important to correctly configure a trailing shield to minimise possible solid-state contamination in any out of chamber AM process, it is somewhat more important that a high quality low oxygen feedstock material is used if the objective is to minimise the oxygen content of the final component produced.

4. Conclusions

This study investigated the effects of different trailing shield configurations on the chemical and tensile properties of Ti-6Al-4V components produced by out of chamber Wire + Arc Additive Manufacturing. Five trailing configurations were studied and ranged from ideal near perfect trailing shielding through to no trailing shield being used. The main findings are as follows:

- Despite the different trailing shield configurations producing various external surface finishes from shiny silver through to flaky brown oxide, this was found to be largely cosmetic and the bulk alloy chemistry, tensile strength and ductility was mostly unaffected and statistically not significant.
- Microhardness testing indicated that the depth of contamination from the external oxidised surface extends no further than 100µm below the exterior surface in the worst case scenario of not using a trailing shield. In the production of engineering components it is very likely that this layer will be removed during machining of the component to final dimensions.
- It was found that the oxygen pickup in the bulk alloys was almost negligible and only notably increased when the trailing shield was removed. Nevertheless, the increase was minor at approximately 0.03wt% (300 ppm) and the bulk oxygen content of the component was well below the maximum required by ASTM Grade 5 and even exceeded the requirements for the higher purity ASTM Grade 23 titanium.
- Providing that no contamination occurs while the metal is molten (i.e. good argon shielding is provided through the deposition torch), the oxygen content is more sensitive to the quality of the wire feedstock used during Wire + Arc Additive Manufacturing as opposed to the design of the trailing shield configuration.

5. Acknowledgments

The authors would like to acknowledge to support of the School of Mechanical and Mining Engineering and the Queensland Centre for Advanced Materials processing and Manufacturing. M.J Bermingham acknowledges the support of the Australian Research Council Discovery Program and is in receipt of Discover Early Career Researcher Award (DE160100260).

6. References

Baufeld, B., Biest, O.V.D., Gault, R., 2010. Additive manufacturing of Ti-6Al-4V components by shaped metal deposition: Microstructure and mechanical properties. Mater. Des. 31, S106-S111.

Baufeld, B., Brandl, E., van der Biest, O., 2011. Wire based additive layer manufacturing: Comparison of microstructure and mechanical properties of Ti–6Al–4V components fabricated by laser-beam deposition and shaped metal deposition. Journal of Materials Processing Technology 211, 1146-1158.

Baufeld, B., Van der Biest, O., 2009. Mechanical properties of Ti-6Al-4V specimens produced by shaped metal deposition. Science and technology of advanced materials 10, 015008.

Bermingham, M.J., Kent, D., Zhan, H., St John, D.H., Dargusch, M.S., 2015. Controlling the microstructure and properties of wire arc additive manufactured Ti-6Al-4V with trace boron additions. Acta Materialia 91, 289-303.

Bermingham, M.J., McDonald, S.D., Dargusch, M.S., 2018. Effect of trace lanthanum hexaboride and boron additions on microstructure, tensile properties and anisotropy of Ti-6Al-4V produced by additive manufacturing. Materials Science and Engineering 719, 1-11.

Brandl, E., Baufeld, B., Leyens, C., Gault, R., 2010. Additive manufactured Ti-6Al-4V using welding wire: Comparison of laser and arc beam deposition and evaluation with respect to aerospace material specifications, Physics Procedia, PART 2 ed, pp. 595-606.

Conrad, H., 1981. Effect of interstitial solutes on the strength and ductility of titanium. Progress in Materials Science 26, 123 - 403.

Dehoff, R.R., Tallman, C., Duty, C.E., Peter, W.H., Yamamoto, Y., Chen, W., Blue, C.A., 2013. Case study: additive manufacturing of aerospace brackets. Advanced Materials and Processes 171.

Ding, J., Colegrove, P., Martina, F., Williams, S., Wiktorowicz, R., Palt, M.R., 2015. Development of a laminar flow local shielding device for wire+arc additive manufacture. Journal of Materials Processing Technology 226, 99-105.

Dobeson, R.G., McDonald, S.D., Dargusch, M.S., 2012. Determination of minimum machining depth after heat treatment of ASTM grade 2 titanium alloy. Advanced Engineering Materials 14, 473-476.

Donachie, M.J., 2000. Titanium a technical guide, Second ed. ASM International, Materials Park, OH.

Froes, F.H., Gungor, M.N., Ashraf Imam, M., 2007. Cost-affordable titanium: the component fabrication perspective. JOM June, 28-31.

Harwig, D.D., Fountain, C., Ittiwattana, W., Castner, H., 2000. Oxygen equivalent effects on the mechanical properties of titanium welds. Welding Journal (Miami, Fla) 79, 305-s.

Hoye, N., Li, H., Norrish, J., Dippenaar, R., 2011. Post-weld atmospheric contamination of gas tungsten arc deposited welds in commercially pure and Ti-6Al-4V titanium alloys, The 12th World Conference on Titanium, p. 4.

Li, X., Xie, J., Zhou, Y., 2005. Effects of oxygen contamination in the argon shielding gas in laser welding of commercially pure titanium thin sheet. Journal of Materials Science 40, 3437-3443.

Maak, P.Y.Y., 1984. The effect of air contamination in the argon sheilding gas on the mechanical properties of titanium gas-tungsten-arc welds. Atomic Energy of Canada Limited.

Mereddy, S., Bermingham, M.J., StJohn, D.H., Dargusch, M.S., 2017. Grain refinement of wire arc additively manufactured titanium by the addition of silicon. Journal of Alloys and Compounds 695, 2097-2103.

Short, A.B., 2009. Gas tungsten arc welding of α + β titanium alloys: a review. Materials Science and Technology 25, 309-324.

Talkington, J., Harwig, D., Castner, H., Joseph, A., Spencer, R., Grimmett, B., 2002. Advances in titanium pipe welding and inspection technology for navy ships. Journal of Ship Production 18, 54-63.

TIMET, 1997. Titanium design and fabrication handbook for industrial applications, p. 37.

Wang, F., Williams, S., Colegrove, P., Antonysamy, A.A., 2013. Microstructure and mechanical properties of wire and arc additive manufactured Ti-6Al-4V. Metallurgical and Materials Transactions A 44, 968-977.

Williams, S.W., Martina, F., Addison, A.C., Ding, J., Pardal, G., Colegrove, P., 2016. Wire + Arc Additive Manufacturing. Materials Science and Technology 32, 641-647.